

Temperature dependent fluctuations in the two-dimensional XY model

S. T. Banks and S. T. Bramwell

Department of Chemistry, University College London, 21 Gordon Street, London WC1H 0AJ, United Kingdom.

E-mail: `simon.banks@ucl.ac.uk`

Abstract. We present a detailed investigation of the probability density function (PDF) of order parameter fluctuations in the finite two-dimensional XY (2d XY) model. In the low temperature critical phase of this model, the PDF approaches a universal non-Gaussian limit distribution in the limit $T \rightarrow 0$. Our analysis resolves the question of temperature dependence of the PDF in this regime, for which conflicting results have been reported. We show analytically that a weak temperature dependence results from the inclusion of multiple loop graphs in a previously-derived graphical expansion. This is confirmed by numerical simulations on two controlled approximations to the 2d XY model: the Harmonic and “Harmonic XY ” models. The Harmonic model has no Kosterlitz-Thouless-Berezinskii (KTB) transition and the PDF becomes progressively less skewed with increasing temperature until it closely approximates a Gaussian function above $T \approx 4\pi$. Near to that temperature we find some evidence of a phase transition, although our observations appear to exclude a thermodynamic singularity.

PACS numbers: 05.40.-a, 05.50,75.10.Hk

Submitted to: *J. Phys. A: Math. Gen.*

1. Introduction

It is often assumed that global measures of many body systems will be normally distributed as a result of the central limit theorem (CLT). This requires that the system be separable into micro- or mesoscopically independent, individually negligible, elements [1]. When these criteria are not met, the CLT is not applicable and there is no reason to expect Gaussian behaviour. A prime example of this comes at equilibrium critical points where the infinite correlation length violates the condition of independence. A universal, non-Gaussian PDF of a global quantity is thus considered to be a signature of criticality and the characterization of the forms of these functions is one of the central problems in the study of critical phenomena [2].

The renormalization group assumes that the PDF of a global measure of a critical system is scale invariant and may thus be obtained from the appropriate critical

fixed point [3–5]. The statistics of critical fluctuations are therefore expected to be the same for all members of a given universality class, as evidenced by studies of Ising [6,7] and Potts [8] models. Conversely there is no reason to assume that systems belonging to different universality classes will possess the same critical PDFs. However in recent years there has been much interest in the fact that experimental and numerical results from diverse systems, that belong to different universality classes, in many cases approximate the distribution of the scalar magnetization in the two-dimensional XY (2d XY) model [9, 10]. This model supports a continuous line of critical points constituting a low temperature critical ‘phase’ that is separated from the paramagnetic region by a Kosterlitz-Thouless-Berezinskii transition [11]. It was observed that the same limit distribution describes the magnetization fluctuations across all the fixed points on the critical line [12] despite the fact that they belong to different universality classes, as can be seen from the temperature dependence of the critical exponents [12, 13].

The practical and theoretical systems that show PDFs of a functional form similar to that of the XY model include power fluctuations in steady state turbulence [9, 10, 14–18] and in liquid crystals undergoing electroconvective flow [19–21], variations in river heights [22], resistance fluctuations near electrical breakdown [23, 24], numerous self-organised critical systems [10, 25–27], dynamical fluctuations in glassy systems [28], and models of equilibrium critical behaviour [29, 30]. Furthermore, the distribution is related to the Fisher-Tippett-Gumbel distribution of extremal statistics [10] which has recently been shown to describe the width fluctuations of periodic, Gaussian, $1/f$ noise [31]. It has been suggested that the apparent universality of the distribution may be explained by the hypothesis that the low temperature or spin wave limit of the 2d XY model captures the essence of critical behaviour for a number of universality classes, with any differences that may occur being hidden by experimental error [9]. More generally, the low temperature limit of the 2d XY model maps on to the two-dimensional Edwards-Wilkinson model, a prototypical model of interface growth. Thus, these results also represent an important application of interface models to the study of fluctuations in complex systems [32].

A team of authors that included one of us analytically derived an integral expression for the 2d XY magnetization PDF in the spin wave regime (sometimes called the BHP function after reference [9]) and indeed found it to be temperature-independent in the large- N limit [13]. This derivation, which applies to the harmonic spin wave approximation to the XY model in the absence of vortices, provides a strong basis for discussions of the apparently universal form of the PDF. In contrast, Palma *et al.* [33] questioned the result of temperature independence. In their analysis of Monte Carlo simulations of the full 2d XY model they found evidence of a weak temperature dependence of the PDF throughout the low temperature phase. However, the full 2d XY model contains both vortex and anharmonic corrections to the harmonic spin wave model; although these are considered irrelevant perturbations, that is not to say that they do not influence the parameters of the PDF in finite systems. It is hard, therefore, to conclude with certainty from numerical studies of the 2d XY model, that the spin

wave contribution itself is temperature-dependent. The aim of the present work was to establish an analytical basis for any possible temperature-dependence in the spin wave regime, and to test it numerically in a controlled manner by means of a series of approximations to the full 2dXY Hamiltonian.

The essential properties of the models investigated are summarised in the following Section (Section 2). Then in Section 3 we present a further analysis of the graphical expansion developed in Ref. [13]. Our numerical results are presented in Section 4. Firstly we simulate the PDF of the Harmonic model, which lacks both metastable vortex configurations and anharmonicities, so is directly comparable with the analytical results. We then simulate the Harmonic XY or HXY Model, in which vortices are re-introduced into the problem. The effect of different definitions of the order parameter is also investigated. Conclusions are drawn in Section 5.

2. The 2dXY Model

The extended critical region of the 2dXY model obviates the need for precision control of external constraints that one associates with locating an isolated critical point [7, 8, 34]. Furthermore the low temperature physics of the model is described precisely by a harmonic Hamiltonian [12, 35, 36] with the result that many properties are exactly calculable, without the need for renormalization or the scaling hypothesis. In the thermodynamic limit the magnetization, m , is zero for all finite temperatures as a result of the destruction of long range order by low energy spin waves – a manifestation of the Mermin-Wagner theorem [37]. However this limit is approached sufficiently slowly for m to remain physically relevant and experimentally observable [38, 39].

The 2dXY model consists of planar spins on a two-dimensional square lattice with nearest neighbour interactions defined by the Hamiltonian

$$H = -J \sum_{\langle \mathbf{r}, \mathbf{r}' \rangle} \cos(\theta_{\mathbf{r}} - \theta_{\mathbf{r}'}). \quad (1)$$

Here J is the (ferromagnetic) exchange interaction, $\theta_{\mathbf{r}}$ is the angle (relative to some arbitrary but fixed axis) made by the spin located at \mathbf{r} and the sum runs over all nearest neighbour pairs of spins. We always deal with a periodic square lattice with sides L , such that $N = L^2$.

Renormalization below the Kosterlitz-Thouless-Berezinskii transition temperature removes vortices from the problem [5, 40] and the model is described by the Harmonic model Hamiltonian [35]

$$H = J \left[1 - \frac{1}{2} \sum_{\langle \mathbf{r}, \mathbf{r}' \rangle} (\theta_{\mathbf{r}} - \theta_{\mathbf{r}'})^2 \right]. \quad (2)$$

This presents a difficulty with regard to the periodicity of the spin variables implicit in (1). The average product of two spin variables defines a Green's function analogous to a propagator of a Euclidean free field. This should be able to take the full range of values between $\pm\infty$ and so the spins in this model are necessarily non-periodic [35].

Intermediate between the Harmonic and full 2dXY models is the HXY model [12], defined by

$$H = \frac{J}{2} \sum_{\langle \mathbf{r}, \mathbf{r}' \rangle} (\theta_{\mathbf{r}} - \theta_{\mathbf{r}'} - 2n\pi)^2. \quad (3)$$

This is numerically simpler than the Villain model [36] as the parameter n is restricted to the values $0, \pm 1$ to ensure that the contents of the brackets remain bounded by $\pm\pi$. As in the full 2dXY model, the spins are defined modulo 2π .

The quantity we study is the instantaneous scalar magnetization, related to the vector order parameter by $m = |\mathbf{m}|$. One definition makes use of the vector spins,

$$m = \frac{1}{N} \sqrt{\left(\sum_{\mathbf{r}} \mathbf{s}_{\mathbf{r}} \right)^2}. \quad (4)$$

We refer to this as the ‘full’ order parameter. A more analytically useful expression defines the magnetization in terms of the spin variables,

$$m = \frac{1}{N} \sum_{\mathbf{r}} \cos \psi_{\mathbf{r}} \quad \text{with} \quad \psi_{\mathbf{r}} = \theta_{\mathbf{r}} - \bar{\theta}. \quad (5)$$

where $\bar{\theta}$ is the instantaneous magnetization direction. For unconfined spins this is the average, $\langle \theta_{\mathbf{r}} \rangle$, for a given configuration. For periodic spins it is convenient to define [12]

$$\bar{\theta} = \frac{\sum_{\mathbf{r}} \sin \theta_{\mathbf{r}}}{\sum_{\mathbf{r}} \cos \theta_{\mathbf{r}}}, \quad (6)$$

which is the same as the mean for large N . Defining ψ enables one to work in a reference frame in which the Goldstone mode has been removed.

At low temperatures angular differences between spins are likely to be small and it may be possible to truncate the cosine in (5). This defines the so-called ‘linearized’ order parameter,

$$m = 1 - \frac{1}{2N} \sum_{\mathbf{r}} \psi_{\mathbf{r}}^2. \quad (7)$$

3. Evaluation of $P(m)$

We are interested in the critical order parameter fluctuations of finite systems which we discuss in terms of probability density functions (PDFs), $P(m)$, calculated in the thermodynamic limit. Thus the order parameter must be correctly normalized to avoid the width of the PDF becoming either zero or infinite as $N \rightarrow \infty$. This has been extensively discussed elsewhere [9, 13] and requires that m be scaled by the standard deviation. We define

$$\Pi(z) = \sigma P(m) \quad z = \frac{m - \langle m \rangle}{\sigma}. \quad (8)$$

3.1. Evaluation of the Moments $\langle m^p \rangle$

A distribution function may be defined in terms of its moments as [41]

$$P(m) = \int_{-\infty}^{\infty} \frac{dx}{2\pi} e^{imx} \sum_{p=0}^{\infty} \frac{(-ix)^p}{p!} \langle m^p \rangle. \quad (9)$$

Following from the definition of the order parameter in equation (5),

$$\langle m^p \rangle = \frac{1}{(2N)^p} \text{Tr} \left\langle \exp \left(\sum_{a=1}^p i\sigma_a \psi_{\mathbf{r}_a} \right) \right\rangle. \quad (10)$$

where i is the imaginary unit and the trace is over all \mathbf{r}_i from 1 to N and all $\sigma_i = \pm 1$. Using Gaussian integration ($\psi_{\mathbf{r}}$ is a Gaussian variable) we can derive [42]

$$\langle m^p \rangle = \left(\frac{\langle m \rangle}{2N} \right)^p \sum_{k=0}^{\infty} \left\{ \frac{1}{k!} \left(-\frac{\tau}{2} \right)^k \text{Tr} \left[\left(\sum_{a \neq b}^p \sigma_a G_{ab} \sigma_b \right)^k \right] \right\} \quad (11)$$

In this expression $\tau = T/J$, G_{ab} is the Green's function propagator function $\tau G(\mathbf{r}_a - \mathbf{r}_b) = \langle \psi_{\mathbf{r}_a} \psi_{\mathbf{r}_b} \rangle$, (a, b) represents all possible pairs of a and b and the shorthand $\sum_{a \neq b} = \sum_a \sum_{b \neq a}$ has been introduced. The upper limits are included explicitly as a reminder that the sums run over p spins, not the entire lattice.

3.2. A Graphical Representation of the Moments

Equation (11) is exact. To proceed further one must develop a means of expressing the sums so that they may either be evaluated precisely, or approximated in a controlled manner. We follow [13] and consider a graphical representation of the moments which allows us to perform well defined partial summations. It is possible to interpret equation (11) diagrammatically by letting G_{ab} represent a line joining two distinct points a and b on a sublattice of p points chosen from the original lattice. The k^{th} term in the argument of the trace is the sum of contributions from all possible graphs with k lines on a sublattice of p points chosen from a parent lattice of size N .

Graphs with lines beginning and ending at the same point are disallowed (by virtue of the constraint $a \neq b$), and graphs with odd vertices (points with an odd number of connections) contribute zero after performing the trace. Contributions from disconnected graphs (those for which the lines do not form a continuous path, e.g. figure 1(c)) are equal to the product of their connected constituents.

Relevant graphs belong to one of two categories: 'Single Loop Graphs' (SLGs) contain only points with no more than two lines attached; 'Multiple Loop Graphs' (MLGs) may have points with any (even) number of lines attached. It has previously been assumed [13] that MLGs do not contribute to the moments of m in the thermodynamic limit. We begin by reviewing the SLG only approach, to show how this yields a temperature independent form of $\Pi(z)$, before returning to consider the validity of neglecting MLGs.

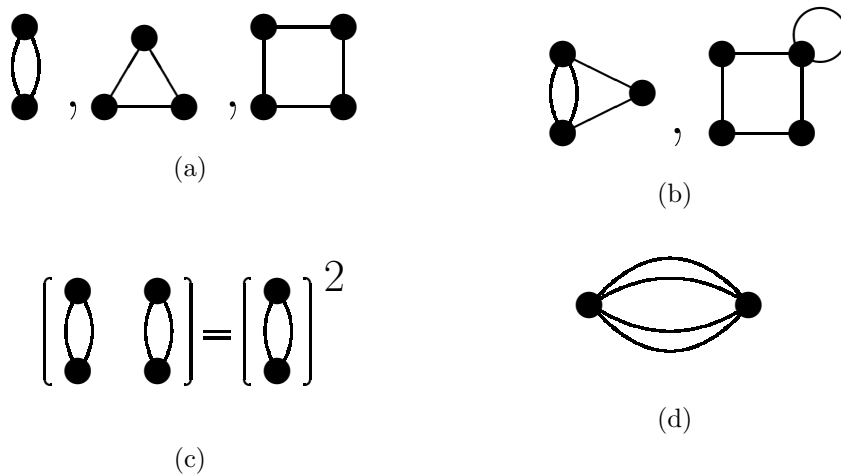


Figure 1. Graphs in the Expansion of $\langle m^p \rangle$: (a) Examples of allowed connected graphs with $p = 2, 3, 4$ and $k = p$. The graphs in (b) are disallowed as they contain either odd vertices or loops involving a single point. (c) An example of a disconnected graph (left hand side) which makes the same contribution as the product of its constituent connected parts. (d) A multiple loop graph.

3.2.1. The Value of Single Loop Graphs Evaluation of (11) requires knowledge of the value of each type of graph and the number of different ways each graph can be created. For connected SLGs it is always possible to rearrange the order of the G_{ab} so that they form a simple closed loop. Transforming to Fourier space using $G(\mathbf{r}) = (1/N) \sum_{\mathbf{q} \neq 0} e^{i\mathbf{q} \cdot \mathbf{r}} G(\mathbf{q})$ then gives an expression for the value of the trace in (11),

$$\begin{aligned} \text{Tr} \left[\left(\sum_{a \neq b}^p \sigma_a G_{ab} \sigma_b \right)^k \right] &= C(k) \frac{2^p}{N^k} \sum_{\mathbf{r}_1=1}^N \cdots \sum_{\mathbf{r}_p=1}^N \sum_{a=1}^p \sum_{b \neq a}^p \cdots \sum_{\mathbf{q}_1 \neq 0} e^{i\mathbf{q}_1 \cdot (\mathbf{r}_a - \mathbf{r}_b)} G(\mathbf{q}_1) \\ &\quad \times \sum_{\mathbf{q}_2 \neq 0} e^{i\mathbf{q}_2 \cdot (\mathbf{r}_b - \mathbf{r}_c)} G(\mathbf{q}_2) \cdots \sum_{\mathbf{q}_k \neq 0} e^{i\mathbf{q}_k \cdot (\mathbf{r}_k - \mathbf{r}_1)} G(\mathbf{q}_k) \quad (12) \\ &= C(k) 2^p {}^p P_k N^p g_k. \quad (13) \end{aligned}$$

The factor $C(k) = 2^{k-1}(k-1)!$ accounts for repetition of topologically identical graphs. The g_k are numerical constants defined by $g_k = (1/N)^k \sum_{\mathbf{q} \neq 0} (1/\gamma_{\mathbf{q}})^k$ with $\gamma_{\mathbf{q}} = G(\mathbf{q})^{-1} = (4 - 2 \cos q_x - 2 \cos q_y)^{-1}$. Evaluation of these constants is discussed in appendix B of reference [13]‡

Adjusting the factor $C(k)$ to account for the extra combinatorial considerations

‡ We note a correction to equation (B3) in reference [13]. The correct expression for g_k is

$$g_k = \frac{1}{4^{k-1} \pi^{2k}} \left\{ \sum_{x=1}^{\infty} \sum_{y=1}^{\infty} \frac{1}{(x^2 + y^2)^k} + \sum_{x=1}^{\infty} \frac{1}{x^{2k}} \right\}.$$

The numerical values that appear elsewhere in that paper are accurate so the error appears to be typographical.

imposed by disconnected graphs leads to [13]

$$\frac{\langle m^p \rangle}{\langle m \rangle^p} = \exp \left(\sum_{k=2}^{\infty} \frac{g_k}{2k} (-\tau)^k \left. \frac{\partial^k}{\partial z^k} z^p \right|_{z=1} \right). \quad (14)$$

The standard deviation is thus $\sigma = \sqrt{g_2/2\tau} \langle m \rangle$, from which it is seen that hyperscaling is obeyed [10,13]. Substituting (14) into (9) and making the transformation $x \rightarrow x/\sigma$ gives the BHP distribution [10,13],

$$P(m) = \int_{-\infty}^{\infty} \frac{dx}{2\pi\sigma} \exp \left\{ \frac{ix(m - \langle m \rangle)}{\sigma} + \sum_{k=2}^{\infty} \frac{g_k}{2k} \left(ix \sqrt{\frac{2}{g_2}} \right)^k \right\}, \quad (15)$$

which is explicitly independent of both system size and temperature. Equation (15), obtained using an SLG only approach, is the main result of [13].

3.3. The Effect of Introducing MLGs

The simplest MLG consists of a sublattice with p points, only two of which are connected by $k > 2$ lines (e.g. Figure 1(d)). Restricting the trace to only this type of graph and again transforming to reciprocal space gives

$$\text{Tr} \left[\left(\sum_{a \neq b}^p \sigma_a G_{ab} \sigma_b \right)^k \right] = 2^{p+k-1} N^p {}^p P_2 \Theta_k \quad (16)$$

where

$$\Theta_k = \frac{1}{N^k} \sum_{\mathbf{q}_1 \neq 0, \dots, \mathbf{q}_k \neq 0} G(\mathbf{q}_1) \dots G(\mathbf{q}_k) \delta \left(\sum_i \mathbf{q}_i \right). \quad (17)$$

The symmetry of $G(\mathbf{q})$ means that $\Theta_2 = g_2$ and so, considering only the additional (MLG) contributions from the highly specific set of graphs discussed here, the second moment becomes

$$\langle m^2 \rangle = \langle m \rangle^2 \left(1 + g_2 \tau^2 + \frac{1}{24} \Theta_k \tau^4 + \dots \right). \quad (18)$$

Therefore in the low temperature limit only the single loop graphs are significant as all MLGs correspond to higher powers of T , however, for high temperatures, contributions from MLGs may not be ruled out.

Substituting $G(\mathbf{q}) = 1/\gamma_{\mathbf{q}}$ into (17), together with the approximation $\gamma_{\mathbf{q}} \approx \mathbf{q}^2$ (representing the greater weight of the low frequency modes), yields, after a little algebra

$$\begin{aligned} \Theta_k &= \frac{1}{(2\pi)^{2k}} \sum_{\{x_i\}=-\infty}^{\infty} \sum_{\{y_i\}=-\infty}^{\infty} \frac{1}{(x_1^2 + y_1^2)} \frac{1}{(x_2^2 + y_2^2)} \times \dots \\ &\times \frac{1}{(x_{k-1}^2 + y_{k-1}^2)} \frac{1}{\left((-\sum_{i=1}^{k-1} x_i)^2 + (-\sum_{i=1}^{k-1} y_i)^2 \right)}. \end{aligned} \quad (19)$$

The sum over $\{x_i\}$ is used to indicate a multiple sum over all members of the set $\{x_1, x_2, \dots, x_k\}$. The terms in this sum are all positive and therefore cannot cancel each other. From this we can see that Θ_k is explicitly non-zero: thus the contributions from MLGs may not be neglected in the thermodynamic limit, contrary to reference [13].

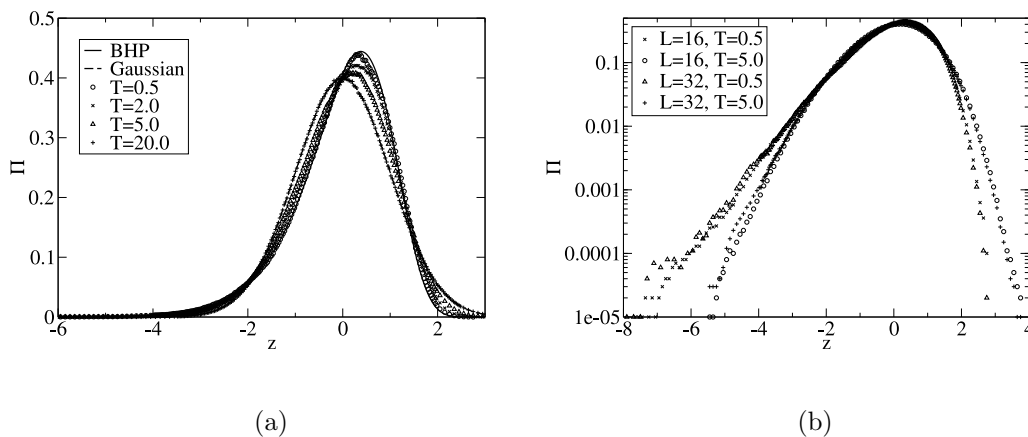


Figure 2. Monte Carlo Simulations on the Harmonic Model. (a) $L = 32$: There is a clear variation with temperature from an approximately BHP form at $T = 0.5$ to a perfect Gaussian by the time $T = 20.0$. (b) Our simulations showed effectively no dependence on system size for $N > 100$. These results are for $L = 16$ and $L = 32$ at $T/J = 0.5, 5.0$. Π and z are as defined in the text.

4. Monte Carlo Simulations

4.1. Simulations of the Harmonic Model

The Harmonic model (2) describes the physics of the critical region of the 2dXY model [11, 40]. Thus if $\Pi(z)$ is independent of T [13] the order parameter fluctuations in the Harmonic model should be BHP like at all temperatures. Single spin-flip Metropolis [43] Monte Carlo simulations were performed on Harmonic systems with $L = 10, 12, 14, \dots, 32$, over a range of temperatures from $T/J = 0.5$ to as high as $T/J = 50$. Equilibration was over 10^6 Monte Carlo steps per spin (MCS/s) with 10^7 MCS/s in total.

The results (figure 2(a)) show a clear variation of $\Pi(z)$ with T (for clarity only the data for $L = 32$ is shown). At low temperatures the distribution is excellently described by the BHP function. However as T increases the PDF becomes progressively less skewed, eventually becoming Gaussian. This is as expected in the light of the work presented in section 3.3. Higher powers of T enter the moment expansion as a result of the inclusion of MLGs. For $r > 2$, σ^r dominates the other moments at high T and the normalized cumulants tend to zero. We observed no variation in the form of the PDF as a function of system size at any temperature, as highlighted in figure 2(b).

The skewness, γ_3 , provides a clear measure of the variation of the PDF with temperature. We have confirmed that γ_3 is independent of N for large systems (though minor corrections to this universality are observed for small N) and a least squares fit to the numerical data (figure 3(a)) reveals that the steady decrease in $|\gamma_3|$ can be

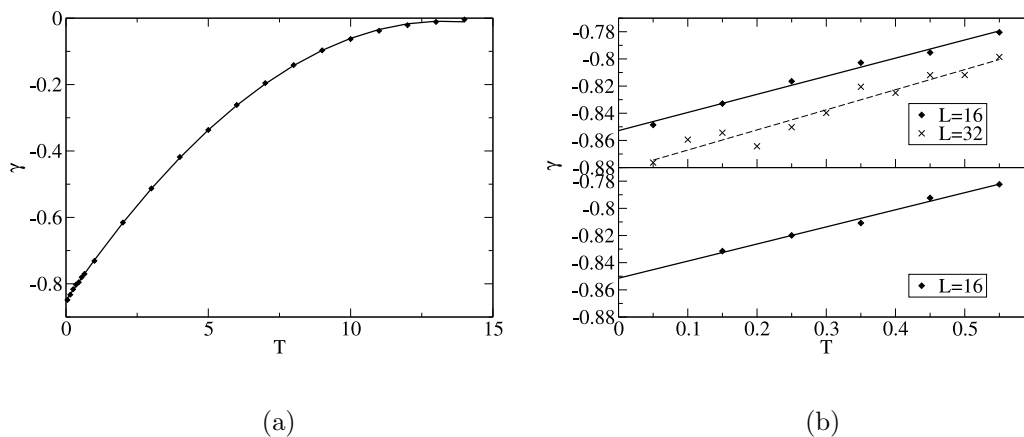


Figure 3. Temperature dependence of the skewness. (a) The Harmonic model with $L = 16$ over a wide range of temperatures. (b) The low temperature region for the Harmonic model (upper plot) with $L = 16$ (diamonds) and $L = 32$ (stars) and the HXY model (lower plot) with $L = 16$, confirming that they obey approximately the same linear relationship in the critical region. The solid and dashed lines are: (a) a least squares quadratic fit; (b) linear regression curves; equations in the text.

approximated (for $L = 16$) by (taking $J = 1$)

$$\gamma_3(T) \approx -0.85 + 0.126T - 0.0048T^2 \quad (20)$$

$$\approx -0.85 + 0.79\eta - 0.19\eta^2, \quad (21)$$

up to the point at which the skewness becomes zero at around $\eta \approx 2$ (here $\eta = T/(2\pi)$ is the spin wave exponent). The zero temperature value of $\gamma_3 = -0.85$ is slightly higher than the theoretical BHP value of $\gamma_3 = -0.89$. We attribute this to the relatively small system used and show in figure 3(b) that increasing the size to $L = 32$ gives a limiting value much closer to the theory with $\gamma_3(T) \approx -0.88 + 0.15T$. We fully expect the true universality with respect to N to be evident for larger systems. However, the skewness is relatively computationally expensive due to the need for averaging and as our results do confirm the evolution of γ_3 with T we leave the determination of the precise form of $\gamma_3(T)$ from larger systems to another time.

4.2. Temperature Dependence in the HXY Model

Renormalization of the HXY model below T_{KT} removes all vortices and recovers the Harmonic model at some, generally higher, temperature. Using the renormalization procedure described by José *et al.* [40] we have calculated the mapping of temperature scales between these two models (table 1) showing that they are coincident below $T \leq 0.9$.

Simulations of the HXY model in this range show a clear change in the skewness of the magnetization distribution as T is varied. Given that there are effectively no

T	K_{eff}	T_{eff}	y
0.1	10	0.1	0.000
0.2	5	0.2	0.000
0.3	3.333	0.3	0.000
0.4	2.5	0.4	0.000
0.5	2	0.5	0.000
0.6	1.667	0.6	0.000
0.7	1.429	0.7	0.000
0.8	1.25	0.8	0.000
0.9	1.111	0.9	0.000
1	0.999	1.001	0.001

T	K_{eff}	T_{eff}	y
1.1	0.905	1.105	0.002
1.2	0.825	1.213	0.004
1.3	0.75	1.333	0.01
1.4	0.677	1.478	0.02
1.5	0.596	1.679	0.038
1.6	0.5	2	0.071
1.7	0.386	2.592	0.129
1.8	0.263	3.804	0.232
1.9	0.157	6.388	0.401
2	0.085	11.74	0.655

Table 1. Equivalent Temperature Scales for the HXY and Harmonic Models with $L = 16$: The temperature of the HXY model is given as T . T_{eff} and K_{eff} are the effective temperature and spin wave stiffness respectively – i.e. relating to the Harmonic model in which all vortices have been renormalized out. The RG expansion parameter y is a measure of the vortex density.

vortices present in the system, it is concluded that the temperature dependence has the same origins as in the Harmonic model, namely the multiple loop graphs in the moment expansion. The plot of $\gamma_3(T)$ for the harmonic model (figure 3(a)) shows an essentially linear dependence at low temperatures. We confirm that a very similar form is observed for the HXY model (figure 3(b)), both $L = 16$ models adhering to

$$\gamma_3 \approx 0.82\eta - 0.85. \quad (22)$$

4.3. The Effect of the Order Parameter

To enable direct comparison with the theoretical predictions all the simulations discussed above have used the cosine form of the order parameter, equation (5). It is interesting to consider the effect on the Harmonic model of substituting for this either the full order parameter, or the much discussed [13] linearized form (7).

4.3.1. The Full Order Parameter High temperature ($T > T_{KT}$) simulations of the 2dXY and HXY models with the cosine order parameter lead to Maxwellian rather than Gaussian magnetization distributions. We suggest that this difference from the Harmonic model is not a consequence of vortices but arises from the constraints placed upon the spin degrees of freedom. The periodicity of the spins forces m to be positive and the PDF is a slice through a two-dimensional Gaussian, appearing as a Maxwell distribution of speeds. A similar result may be obtained for the harmonic model by using the full order parameter (4). This quantity is necessarily positive and thus has the same effect as constraining the spin variables to within the positive range of the cosine function in (5). Monte Carlo simulations confirm this, showing BHP fluctuations changing to Maxwellian behaviour as T is increased (figure 4). Despite the Harmonic model/full order parameter combination giving the same limiting T PDFs as the 2dXY and HXY models, it should be noted that the path of intermediate distributions is different and only for the Harmonic model is there a region of Gaussian behaviour.

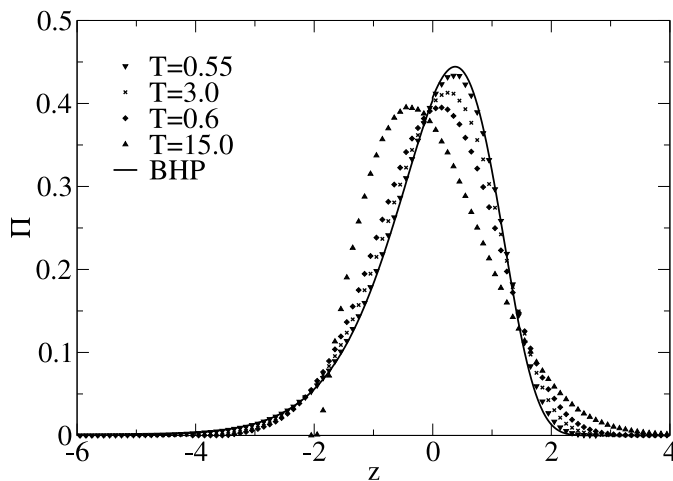


Figure 4. Monte Carlo Results for the Harmonic Model with Full Order Parameter ($L = 16$): Again there is a clear variation of the distribution as a function of temperature. At low T the curve closely approximates the BHP form, but with the full order parameter it becomes Maxwellian, rather than Gaussian, at high T (c.f. figure 2(a)).

4.3.2. The Linearized Order Parameter The linearized order parameter (7) only describes m at temperatures low enough to exclude large angular differences between neighbouring spins. Despite this, Bramwell *et al.* demonstrated that, for the Harmonic model, the distribution of the linearized order parameter is precisely the BHP function at all temperatures [13]. We have simulated this model for a system with $N = 1024$ and the results confirm that the magnetization distribution is consistently of the BHP form for all our simulations, even up to $T/J = 50$. This result may now be understood as a manifestation of the low temperature approximation implicit in the derivation of the BHP distribution (15) [13]. The neglect of MLGs leads to a PDF which perfectly describes critical fluctuations in the 2dXY model, but strictly only in the limit $T \rightarrow 0$. The linearized OP is only a valid description of the magnetization in the same limit and hence has the same temperature independent fluctuations as the full OP at $T = 0$. We emphasize that we have not demonstrated an analytical equivalence between the neglect of MLGs and the neglect of anharmonic terms in the cosine OP. Despite this it seems likely that this heuristic justification of the rigorous equivalence between the PDFs obtained in each case is correct.

5. Is There A Phase Transition in the Harmonic Model?

The change from non-Gaussian to Gaussian statistics in our Harmonic model simulations is reminiscent of a Kosterlitz-Thouless-Berezinskii transition from a critical region to a

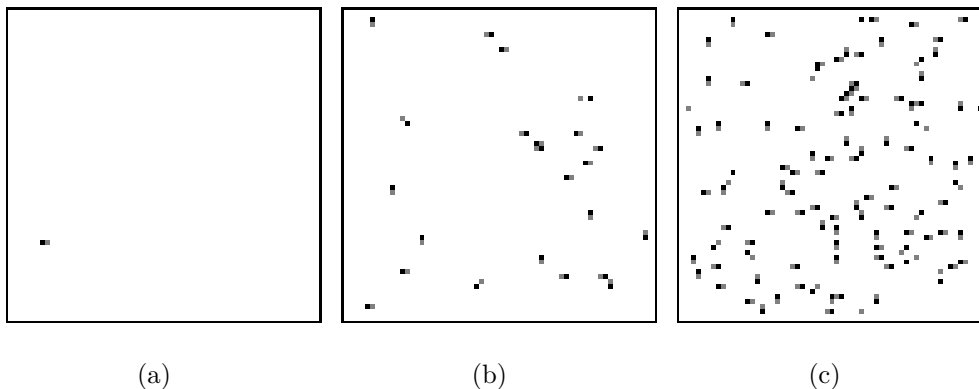


Figure 5. Vortices in the Harmonic Model: These figures are snapshots of the Harmonic model with $N = 3600$ at (a) $T/J = 1.5$, (b) $T/J = 2.5$, and (c) $T/J = 3.5$. At low temperatures one sees the surprising emergence of a tightly bound vortex/anti-vortex pair. The vortex density increases with T and despite a small degree of separation of some pairs in (b) and (c), isolated vortices are not observed. The grey squares represent a vorticity of -1 , the black squares a vorticity of $+1$.

paramagnetic phase [44]. The temperature at which Gaussianity is first observed ties in with the expression for the susceptibility derived in [12]

$$\chi = \frac{N \langle m \rangle^2 T}{2a_{2d} J^2} \sim N^{1-T/4\pi J} \quad (23)$$

($a_{2d} \approx 258.6$) which has χ diverging only for $T/J < 4\pi$. There is, however, no change in the behaviour of the magnetization as one passes through this point as one would expect for a true phase change and it must be remembered that (23) is only approximate [12].

The KT transition is associated with the onset of topological order, which suggests that, if such a transition were to occur in the Harmonic model, a suitable topological defect must be found. We have identified one such defect, and, rather surprisingly, it is a spin vortex. The definition of a vortex is complicated by the non-periodicity of the spins. We assign a ‘winding number’ to each pair of spins equivalent to the multiple of 2π that must be subtracted from their difference to give a value in the range $\pm\pi$. The sum over the winding numbers around a closed path is then the vorticity of the enclosed region. In a system with $N = 3600$ we observe a tightly bound vortex/anti-vortex pair at $T/J = 1.5$ (figure 5). It appears as though the vortices are created by the superposition of high energy spin waves, in contradiction to the assumption that spin waves and vortices are independent [35,44] (although, as previous studies have generally focused on temperatures far below T_{KT} this should have no bearing on their results). The vortex density increases with T , eventually becoming so large that it is difficult to distinguish individual pairs. At no point do any vortices have a vorticity greater than 1 and isolated vortices are never observed.

The lack of vortex pair unbinding can be explained by considering the free energy of an isolated vortex. Adapting the standard calculation (see, for example, [45]) to allow

for the non-periodic spins, we arrive at an expression for the energy of a vortex,

$$E_{\text{vor}} = 2J\pi^2(L - a) - J\pi l \ln\left(\frac{L}{a}\right), \quad (24)$$

where l is a constant of the order of the lattice spacing a . That E_{vor} diverges as \sqrt{N} means that it dominates the entropy (which diverges logarithmically with N) at all temperatures. Thus isolated vortices are always energetically unstable in the Harmonic model. Bound pairs of vortices whose cores are separated by a distance R will have

$$E_{\text{vor-pair}} \sim \mathcal{O}(R - \ln(R)) \quad (25)$$

and are therefore feasible provided R remains small.

Despite the observation of topological defects, the evidence from statistics and the behaviour of the susceptibility, the lack of vortex-pair unbinding must lead to the conclusion that no Kosterlitz-Thouless-Berezinskii transition occurs in the Harmonic model.

6. Conclusion

In this work we have considered the PDF of order parameter fluctuations in the finite 2dXY model in the spin wave approximation. We have not generally considered the effect of spin vortices on the PDF. Bound vortex pairs are irrelevant perturbations in the low temperature phase and so might be expected to leave the PDF unaltered, but this has not been proved explicitly. For a study of the effect of vortex unbinding on the PDF, see [14].

The original result of [13] suggested a PDF describing magnetization fluctuations in critical finite 2dXY magnets which was truly universal and had been seen to describe the statistics of a range of critical systems. We have demonstrated analytically that there is in fact a temperature dependence and so it must be concluded that strict universality does not hold. However, numerical work shows that the effect of temperature is very weak. From a visual point of view the distribution looks very similar across the critical, vortex free, region. The temperature dependence established here is weaker than, but of the same magnitude as, that claimed by Palma *et al.*, for the full XY model [33]. More work is needed to fully understand this difference.

Despite the weakness of the temperature dependence, we feel that the confirmation of its existence is an important result, particularly as much literature has grown up around the unusual behaviour of fluctuations in the 2dXY model. Significantly it has been shown that the equivalence between the distributions obtained using the cosine and linearized order parameters in [13] is the result of the imposition of low temperature in both cases – by neglect of MLGs and anharmonic terms respectively.

We note that the assertion that the Harmonic model is ‘vortex free’ is true only in the sense that vortices do not appear explicitly in the Hamiltonian. However, by introducing a definition of vortices consistent with infinitely variable spins, we have identified tightly bound vortex pairs at high temperatures which we conclude are the

result of the superposition of high energy spin waves. The crossover to a Gaussian statistical regime at $T \approx 4\pi$ for the Harmonic model, coupled with the fact that the susceptibility appears not to diverge above this point, are suggestive of a Kosterlitz-Thouless-Berezinskii transition. However, the unbinding of vortex pairs this requires is not observed and we argue that isolated vortices in this model are not energetically viable.

Acknowledgments

It is a pleasure to thank P. C. W. Holdsworth, Z. Rácz and M. Clusel for useful discussions. S. T. Banks thanks the UCL Graduate School for funding through a Graduate School Research Scholarship.

References

- [1] Landau L D and Lifshitz E M 1980 *Statistical Physics* vol 1 (Pergamon)
- [2] Wilson K G and Kogut J 1974 *Phys. Rep.* **12** 75
- [3] Cassandro M and Jona-Lasinio G 1978 *Adv. Phys.* **27** 913
- [4] Garrod C 1995 *Statistical Mechanics and Thermodynamics* (Oxford University Press)
- [5] Cardy J 1996 *Scaling and Renormalization in Statistical Physics* (Cambridge University Press)
- [6] Bruce K 1981 *J. Phys. C* **14** 3667
- [7] Binder K P 1992 in *Computational Methods in Field Theory – Lecture Notes in Physics* vol 490 ed H Gausterer and C B Lang (Springer-Verlag)
- [8] Botet R and Ploszajczak M 2000 *Phys. Rev. E* **62** 1825
- [9] Bramwell S T, Holdsworth P C W and Pinton J-F 1998 *Nature* **396** 552
- [10] Bramwell S T, Christensen K, Fortin J-Y, Holdsworth P C W, Jensen H J, Lise S, López J, Nicodemi M, Pinton J-F and Sellitto M 2000 *Phys. Rev. Lett.* **84** 3744
- [11] Kosterlitz J M 1974 *J. Phys. C: Solid State Phys.* **7** 1046
- [12] Archambault P, Bramwell S T and Holdsworth P C W 1997 *J. Phys. A: Math. Gen.* **30** 8363
- [13] Bramwell S T, Fortin J-F, Holdsworth P C W, Peysson S, Pinton J-F, Portelli B and Sellitto M 2001 *Phys. Rev. E* **63** 2001
- [14] Holdsworth P C W and Sellitto M 2002 *Physica A* **315** 643
- [15] Portelli B, Holdsworth P C W and Pinton J-F 2003 *Phys. Rev. Lett.* **90** 104501
- [16] Peyrard M 2004 *Physica D* **193** 265
- [17] Peyrard M and Daumont I 2002 *Europhys. Lett.* **59** 834
- [18] Noullez A and Pinton J-F 2002 *Eur. Phys. J. B* **28** 231
- [19] Toth-Katona T and Gleeson J T 2004 *Phys. Rev. E* **69** 016302
- [20] Toth-Katona T and Gleeson J T 2003 *Phys. Rev. Lett.* **91** 264501
- [21] Goldburg W I, Goldschmidt Y Y and Kellay H 2001 *Phys. Rev. Lett.* **87** 245502
- [22] Bramwell S T, Fennel T, Holdsworth P C W and Portelli B 2002 *Europhys. Lett.* **57** 310
- [23] Pennetta C, Alfinito E, Reggiani L and Ruffo S 2004 *Semicond. Sci. Technol.* **19** S164
- [24] Pennetta C, Alfinito E, Reggiani L and Ruffo S 2004 *Physica A* **340** 380
- [25] Sinha-Ray P, de Agua L B and Jensen H J 2001 *Physica D* **157** 186
- [26] Dahlstedt K and Jensen H J 2001 *J. Phys. A: Math. Gen.* **34** 11193
- [27] Chapman S C, Rowlands G and Watkins N W 2003 *Nonlin. Proc. Geoph.* **9** 409
- [28] Chamon C, Charbonneau P, Cugliandolo L F, Reichman D R and Sellitto M 2004 *J. Chem. Phys.* **121** 10120
- [29] Clusel M, Fortin J-Y and Holdsworth P C W 2004 *Phys. Rev. E* 046112

- [30] Zheng B 2003 *Phys. Rev. E* **67** 026114
- [31] Antal T, Droz M, Gyögyi G and Rácz Z 2001 *Phys. Rev. Lett.* **87** 240601
- [32] Rácz Z and Plischke M 1994 *Phys. Rev. E* **50** 3530
- [33] Palma G, Meyer T and Labbé R 2002 *Phys. Rev. E* **66** 026108
- [34] Binder K 1981 *Z. Phys. B* **43** 119
- [35] Berezinskiĭ V L 1971 *Sov. Phys. JETP* **32** 493
- [36] Villain J 1975 *J. Physique* **36** 581
- [37] Mermin N D and Wagner H 1966 *Phys. Rev. Lett.* **17** 1133
- [38] Bramwell S T and Holdsworth P C W 1993 *J. Phys.: Condens. Matter* **5** L53
- [39] Bramwell S T and Holdsworth P C W 1994 *Phys. Rev. B* **49** 8811
- [40] José J V, Kadanoff L P, Kirkpatrick S and Nelson D R 1977 *Phys. Rev. B* **16** 1217
- [41] Kendall M, Stuart A and Ord J K 1987 *Kendall's Advanced Theory of Statistics* vol 1 (London: Griffin)
- [42] Archambault P, Bramwell S T, Fortin J-Y, Holdsworth P C W, Peysson S and Pinton J-F 1998 *J. App. Phys.* **83** 7234
- [43] Metropolis N, Rosenbluth A, Rosenbluth M, Teller A and Teller E 1953 *J. Chem. Phys.* **21** 1087
- [44] Kosterlitz J M and Thouless D J 1973 *J. Phys. C: Solid State Phys.* **6** 1181
- [45] Chaikin P M and Lubensky T C 1995 *Principles of Condensed Matter Physics* (Cambridge University Press)